Research Article

Performance Assessment of Solar Air Heater Channel with Inclined Groove Turbulators

N. Koolnapadol[1]
P. Promvonge[2]
C. Khanoknaiyakarn[3]
P. Promthaisong[4]
P. Hoonpong[5]
A. Chaimanatsakun[6]
S. Gururatana[6]
S. Skullong[6,*]

[1] *Department of Automotive Mechanical Engineering, Faculty of Industrial Technology, Rajabhat Rajanagarindra University, Chachoengsao 24000, Thailand*
[2] *Department of Mechanical Engineering, School of Engineering, King Mongkut's Institute of Technology Ladkrabang, Bangkok 10520, Thailand*
[3] *Division of Engineering Management, Graduate School, Southeast Asia University, Bangkok 10160, Thailand*
[4] *Heat Pipe and Thermal Tool Design Research Unit (HTDR), Faculty of Engineering, Mahasarakham University, Maha Sarakham 44150, Thailand*
[5] *Department of Mechanical Technology, Faculty of Industrial Technology, Thepsatri Rajabhat University, Lopburi 15000, Thailand*
[6] *Department of Mechanical Engineering, Faculty of Engineering at Sriracha, Kasetsart University Sriracha Campus, Chonburi 20230, Thailand*

Abstract:
An experimental investigation was carried out to explore the thermal performance and frictional loss features in a solar air heater (SAH) channel that was intentionally roughened on the absorber surface using multiple inclined groove turbulators. The working fluid, air, flows into the SAH channel, which has a consistent surface heat flux for Reynolds numbers (Re) varying between 5290 and 22,600 in the current research. Thermal characteristics at a single inclination angle ($\alpha = 45°$) are investigated in this research by comparing the effects of three distinct relative groove frequencies (P/H=PR=0.8, 1.2 and 1.6) and groove depth ratios (D/H=DR=0.16, 0.24 and 0.32). The findings highlight that the employ of inclined grooves results in a noticeable rise in Nusselt number (Nu) from 1.24 to 2.82 times relative to the smooth absorber plate (smooth channel), as well as a 1.88 to 7.9 times increase in friction factor (f). The Nu and f show an increasing trend when Re increases, whereas the opposite pattern occurs as DR and PR increase. At PR = 0.8 and DR = 0.32, the inclined groove roughness has the largest thermal effectiveness factor (TEF) of around 1.64. The Nu and f correlations, which are functions of inclined groove features, have also been established.

Keywords: *Heat transfer, Solar air heater, Thermal performance, Inclined groove*

1. Introduction

Numerous solar energy/power technologies are being developed to produce clean, renewable energy. Some of these systems can generate electricity by converting solar radiation into thermal energy at high temperatures in gas or steam, which may then be used to power an electrical generator's turbine.

There have been suggestions that adding a turbulator device can improve solar thermal systems' thermal performance. One of the best ways to use solar energy for thermal applications on a big scale is with a solar air heater (SAH). SAH has found widespread application in the engineering and agricultural industries, including crop drying, space heating, heat exchangers, and more [1-15]. A typical SAH has an airflow channel, insulation, a glass cover, and a smooth absorber plate to collect solar radiation, as seen in Figure 1. The typical absorber plate of SAH generally has very poor thermal performance owing to the boundary layer formation close to the absorber surface, which results in a low convection coefficient. To break down the boundary layer that establishes on the surface of the absorber, one can incorporate rib and groove turbulators on the ground side of the absorber [16-18]. This can result in an increased convection coefficient on the surface of the absorber. According to several studies, increasing the artificial roughness of the heated surface in the form of a rib or groove will speed up the transfer of heat.

Taslim et al. [19] employed a liquid crystal approach to analyze the behavior of air flow, friction, and temperature in a SAH channel fitted with rectangular rib turbulators. Their findings indicated that the heat transmission improved as the relative rib height (e/H) climbed, and they determined that the optimal e/H was between 0.083 and 0.125. Yadav and Bhagoria [20] employed two-dimensional computational fluid dynamics (CFD) to investigate a SAH channel that contained ribs with delta cross-sections positioned on the absorber. They discovered that placing the delta ribs on the absorber produced the largest Nu and f values, which were around 3.073 and 3.356 times greater than the smooth-plate channel, respectively. Kumar et al. [21] employed an absorber plate with multiple V-shaped ribs separated by a gap. In comparison to the smooth absorber plate, they discovered that introducing this artificial roughness raised Nu and f by roughly 6.74 and 6.37 times, respectively.

Most dimple/groove turbulators have been frequently used to increase the thermal performance of heat exchangers and SAH systems due to their relatively low friction loss when compared to other choices. Rashidi et al. [22] investigated the effect of dimple or groove roughness on heat transmission, friction loss, and velocity distribution. They noted that protrusion walls generate more friction loss than dimpled or grooved walls when utilized in heat exchangers or SAH systems because they make it more difficult for the flow to pass through. Sethi et al. [23] examined the potential of dimple-shaped roughness components on the absorber plate to enhance heat transfer in a SAH duct for Re varying from 3600 to 18,000. They discovered that the dimpled form roughness, with a roughness pitch ratio, $p/e = 10$, had the fastest heat transmission rate. Jin et al. [24] performed an experimental work to explore heat transmission phenomena in the case of pulsing channel flow in a triangular grooved duct. According to the findings, the heat transmission augmentation was around 350% exceeding the steady flow. Eiamsa-ard and Promvonge [25] utilized numerous turbulence models (standard k−ω, standard k−ε, RNG k−ε, and SST k−ω) to evaluate the boost of heat transmission in a channel having periodical grooves on one wall. The grooved channel demonstrated a peak thermal performance of approximately 1.33. Furthermore, the turbulent model of RNG k−ε was preferable for estimating heat transfer and fluid flow in the grooved channel.

Luo et al. [26] numerically examined in a SAH channel the impact of dimple configurations on heat transmission and flow structure. A dimple coupled with a delta winglet provided a thermal performance roughly 28.50% more than the conventional SAH. Chokphoemphun et al. [27] investigated the thermal performance of a single-pass SAH channel with grooves experimentally. They showed the impacts of the groove's inclination angles (α = 30° and 45°), groove depth (d = 4, 6 and 8 mm), for various Reynolds numbers (6700 to 17,000). In contrast to the smooth channel, they discovered that the heat transmission rate rose by a factor of 1.32-2.00 and the friction loss increased by a factor of 1.25-33.83. In addition, a groove depth of only 8 mm was sufficient to attain a maximum TEF of 1.49. On heat transmission and fluid flow structure in rectangular convex-dimple-grooved channels, Zhang et al. [28] performed CFD studies. Their solver was the commercially produced CFD code ANSYS CFX. Turbulent airflow via convex-dimple-grooved channels was simulated using the SST turbulence model. The surface with convex-dimple-grooves showed a thermal effectiveness with a maximal value of 1.29 and a significantly smaller frictional loss than the surface with transverse circular-protrusion grooves, according to their report. Table 1 shows the Grooved Channel configurations derived from the above literature analysis.

The literature review above indicates that the use of dimples/grooves is more appealing than rib turbulators due to their reduced friction loss. Typically, designers incorporate dimples or grooves into their designs to heighten turbulence, which in turn can improve the rate of heat transmission while reducing frictional loss. Nevertheless, the grooves in the literature review are arranged in a 90° transverse orientation to the air flow. Therefore, the objective of this investigation is to investigate the manner in which the inclined groove functions as a vortex generator in a channel to enhance heat transmission and flow patterns in an area with turbulent flow (Re = 5290–22,600). The

primary objective of the current work is to enhance the thermal effectiveness and heat transmission rate of a SAH channel by employing the new design absorber plate, which is characterized by inclined grooves. The inclined grooved absorber plate's investigated parameters include three relative groove pitches (P/H =PR=0.8, 1.2 and 1.6) and groove depth ratios (D/H=DR=0.16, 0.24 and 0.32) at a single inclination angle ($\alpha = 45°$).
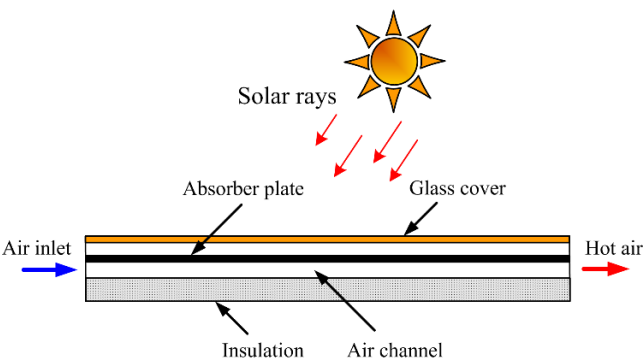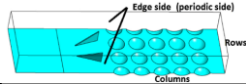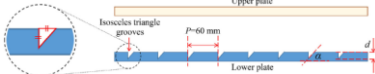

Fig. 1. Conventional solar collector.

Table 1: Summaries of dimple/groove turbulators used in a SAH channel.

Authors and test section	Results		
	Nu/Nu_0	f/f_0	TEF_{max}
Rectangular groove, Eiamsa-ard and Promvonge [25]	-	-	1.33
Dimple and delta winglet, Luo et al. [26]	1.7	2.2	1.46
Triangular groove, Chokphoemphun et al. [27]	2	3.9	1.49
Rectangular convex-dimple-groove, Zhang et al. [28]	1.35	1.9	1.29

2. Experimental system

Figure 2 depicts a diagram of the experimental configuration of the SAH system. The experiment included the flow of cold air at typical environmental conditions through the test channel, with Reynolds numbers (Re) varying from 5290 to 22,600. The volumetric airflow rate was determined using a plate called an orifice constructed in accordance with ASME standard [29]. The orifice plate was calibrated using a vane-type/hot-wire anemometer (Testo 480) to gauge the airflow velocities along the pipe section. An electrical heater sheet was connected to the absorber plate in the test channel to generate a constant surface heat flux of approximately 3000 W/m². This heat flux was maintained by an AC power source, namely a variac transformer. The test channel's exterior surface was effectively insulated to reduce convective heat loss to the environment around it. Following the settling tank, the channel had a calm portion (2200 mm), a test section (800 mm), and an exit (300 mm). The test channel, consisting of an aluminum plate, has a width (W) of 200 mm, a thickness (t) of 12 mm and a channel height (H) of 25 mm. RTD-type (Pt100) temperature sensors were placed at both ends of the test channel to monitor the temperature of the bulk air entering and exiting the channel. Additionally, 30 thermocouples (T-type) were placed on the top wall of the test section to detect the surface temperature of the absorber plate (T_a). The thermocouples were utilized to gauge the change in temperature across the absorber plate in order to estimate the average surface temperature. The Fluke 2680A data collecting system consistently captured and stored all temperature measurements from the measurement instrument. The pressure drops over the grooved absorber plate were recorded as well using a Dwyer (475-1-FM 475 Mark III) digital manometer.

The standards and criteria followed for channel design, which includes the entry section, the test section, and the exit section, as mentioned in Refs. [30,31].

The uncertainty in the estimation of the measurements was described in Ref. [32]. It was estimated that the uncertainties in pressure, velocity, and temperature readings were within ±4.5%, ±3.5% and ±0.1%, respectively. For Nu, f and Re, the greatest uncertainties of the dimensionless parameters were ±4.3%, ±5.5% and ±3.3%, correspondingly. Measurements of the smooth channel and the inclined-grooved plate were repeatable within the previously identified uncertainty areas.
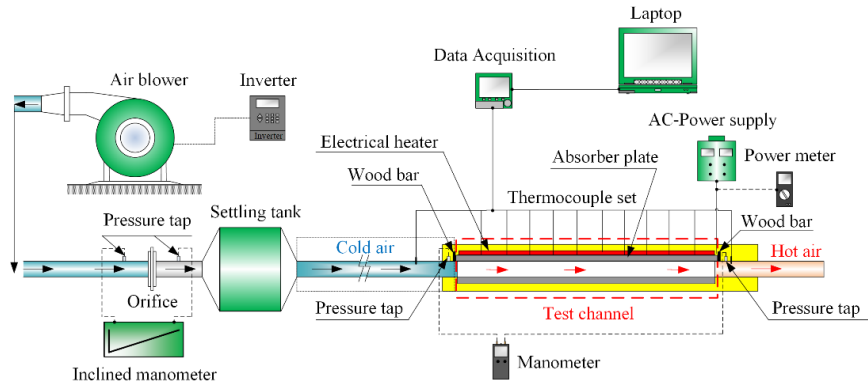

Fig. 2. Schematic diagram of experimental setup for SAH system.

The selected absorber plate geometry, which includes both smooth and grooved surfaces, is schematically shown in Figure 3. The aluminum flat plate was created using a 12-mm-thick (t) slab. Wire-EDM (electrical discharge machine) cutting made grooved plates that are 4 mm, 6 mm and 8 mm deep, which means that the groove depth ratios (D/H=DR) are 0.16, 0.24 and 0.32. As shown in Figure 3(b), grooves of 3 mm in width (w) were milled using a 45° groove chamfer ($\alpha = 45°$). At a single inclination angle (α) of 45°, there were three longitudinal pitch spacings (P = 20 mm, 30 mm and 40 mm), which corresponded to relative groove-pitches (P/H = PR) of 0.8, 1.2 and 1.6.
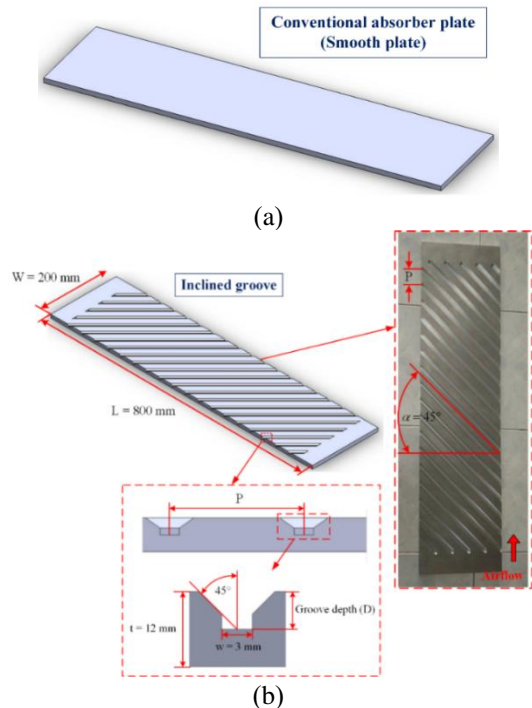

Fig. 3. Test section with (a) smooth plate and (b) inclined-grooved plate.

3. Theoretical analysis

The convective heat transmission between the absorber surface and flowing air of an inclined groove SAH channel is being evaluated in the current research. Interested characteristics are relative groove pitch (PR), Reynolds number (Re) and groove depth ratio (DR). Given the channel hydraulic diameter, D_h, the Reynolds number is computed via

$$\text{Re} = U \times D_h / \nu \tag{1}$$

where D_h is denoted by

$$D_h = (4 \times W \times H) / 2 \times (W + H) \tag{2}$$

The pressure difference is adopted to calculate f (friction factor) as follows:

$$f = \frac{2}{(L/D_h)} \times \frac{\Delta P}{\rho \times U^2} \tag{3}$$

where U represents the average velocity of the air.

Air moved through the SAH channel in the experiment under a consistent wall heat flux. Assuming that the heat loss from the test section is equivalent to the rate of heat transmission at the steady state, expressed as:

$$\dot{Q}_{air} = \dot{Q}_{conv} \tag{4}$$

where

$$\dot{Q}_{air} = \dot{m} \times C_p \times (T_{out} - T_{in}) = V \times I - \dot{Q}_{loss} \tag{5}$$

The convection coefficient inside the test channel is evaluable from

$$\dot{Q}_{conv} = h \times A \times (\tilde{T}_a - T_b) \tag{6}$$

where A denotes the absorber plate surface area and defined as

$$A = L \times W \tag{7}$$

in which

$$T_b = (T_{out} + T_{in}) / 2 \tag{8}$$

and

$$\tilde{T}_a = \sum T_a / 30 \tag{9}$$

where T_a stands for the absorber's local temperature, which is uniformly distributed along the test channel's surface. One estimates the mean heat transfer coefficient (h) as follows:

$$h = \dot{m} \times C_{p,air} \times (T_{out} - T_{in}) / A \times (\tilde{T}_a - T_b) \tag{10}$$

The mean Nusselt number is obtainable from

$$\text{Nu} = h \times D_h / k \tag{11}$$

At mean bulk temperature of air (T_b) in Eq. (8), all thermophysical characteristics of air are evaluated.
Using an equal blowing power, the thermal performance of the grooved absorber plate is assessed relative to the smooth absorber plate using a thermal enhancement factor (TEF) as described by Refs. [30,31] stated as

$$\text{TEF} = (\text{Nu}/\text{Nu}_0) / (f/f_0)^{0.8/2.75} \tag{12}$$

in which the subscript "0" is for the smooth absorber only.

4. Results and discussion

4.1. Verification of smooth absorber plate

Using the SAH channel with grooved and smooth absorber plates, the present study shows experimental data on heat transmission and frictional loss.

The current measurement results on the heat transmission characteristics and frictional loss inside a smooth absorber plate are initially validated in the form of the friction factor (f) and Nusselt number (Nu). The values for this smooth-plate absorber are contrasted to the Gnielinski, Dittus-Boelter, Petukhov and Blasius correlations pertaining to turbulent flow in channels that are available in the open literature [33].

Equations of Petukhov,

$$f = (0.79 \ln \mathrm{Re} - 1.64)^{-2} \tag{13}$$

Blasius,

$$f = 0.316 \, \mathrm{Re}^{-0.25} \tag{14}$$

Gnielinski,

$$\mathrm{Nu} = \frac{(f/8)(\mathrm{Re} - 1000)\mathrm{Pr}}{1 + 12.7(f/8)^{1/2}(\mathrm{Pr}^{2/3} - 1)} \tag{15}$$

and Dittus-Boelter (for heating),

$$\mathrm{Nu} = 0.023 \, \mathrm{Re}^{0.8} \mathrm{Pr}^{0.4} \tag{16}$$

The contrasts of the current f and Nu of the smooth channel with data of equations (13) to (16) are exhibited in Figure 4(a) and (b). The correlation and experimental data exhibit discrepancies of ±7.5% and ±6.7% for Eqs. (13) and (14) and ±5.3% and ±4.5% for Eqs. (15) to (16), respectively. There is strong agreement between the measurements and the correlations reported in the literature, in the image.
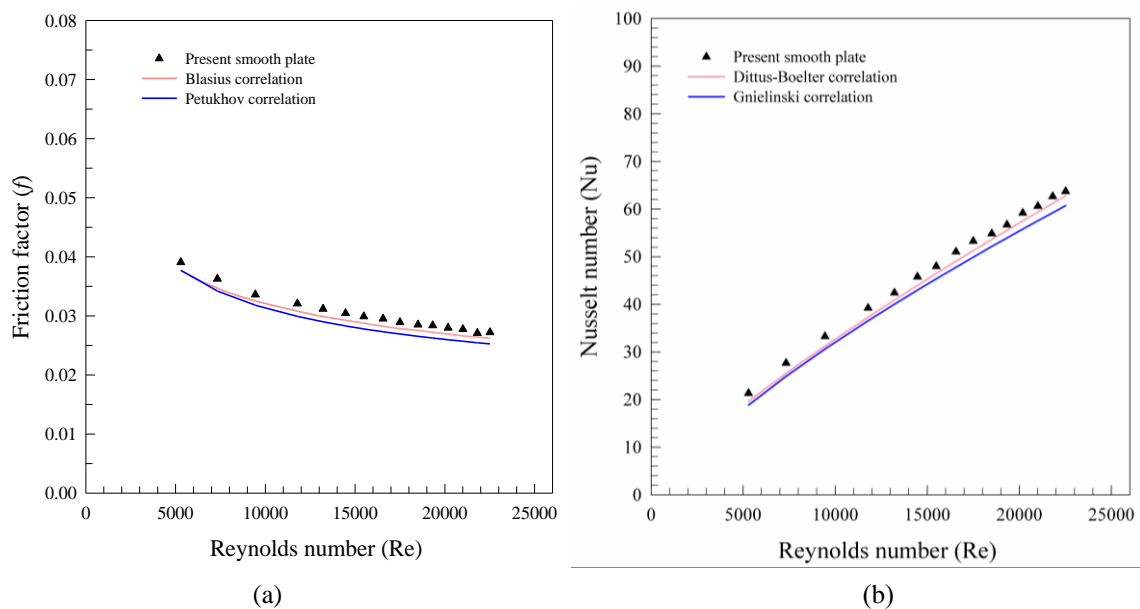

(a)   (b)

Fig. 4. (a) f and (b) Nu comparison with correlation's data for the smooth absorber plate.

4.2 Axial wall and fluid temperature variations in the test channel

Figure 5 illustrates the axial variations in wall temperatures (T_w) of the absorber and temperatures of air ($T_{air,inlet}$ and $T_{air,outlet}$) across the SAH channel incorporating a 45° inclined groove for DR values of 0.32, 0.24 and 0.16 at PR = 0.8 and Re = 9445, with x representing the location of thermocouples commencing from the entrance of the test section. In the image, T_w demonstrates an upward trend as x/H increases across all DR scenarios, with a minor decline of the final two positions at $x/H = 31$ and 28 attributed to radiation effect at the outlet. The minimum value for the wall temperature is obtained when the DR is 0.32, as the maximum air temperature in the exit region is achieved because of increased heat extraction from the absorber surface. The error bars for the three quantities of DR are shown in Figure 5 and the experimental results for the wall and air temperatures were consistent under the range of uncertainty limits.
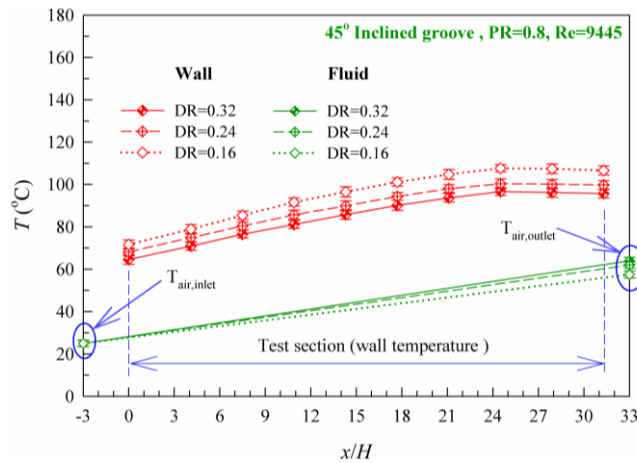

Fig. 5. Variations of air and wall temperatures inside the tested channel with inclined grooves.

4.3 Thermal behaviors

Figure 6(a) and (b) depicts the changes in Nu and Nu/Nu$_0$ ratio as functions of Re values when utilizing 45° inclined grooves. Figure 6(a) clearly demonstrates that the heat transmission (represented by Nu) grows as Re rises. A flat-plate channel (with no groove) displays a much lower Nu than the SAH channel with an inclined-grooved absorber. The grooved absorber plate outperforms the smooth one in terms of Nu by a factor of 25–182%, with the maximum Nu increase seen at DR=0.32 and PR=0.8. This suggests that the convection heat transmission process can be boosted by the disruptive boundary layer and reverse/recirculation flow from the inclined groove.
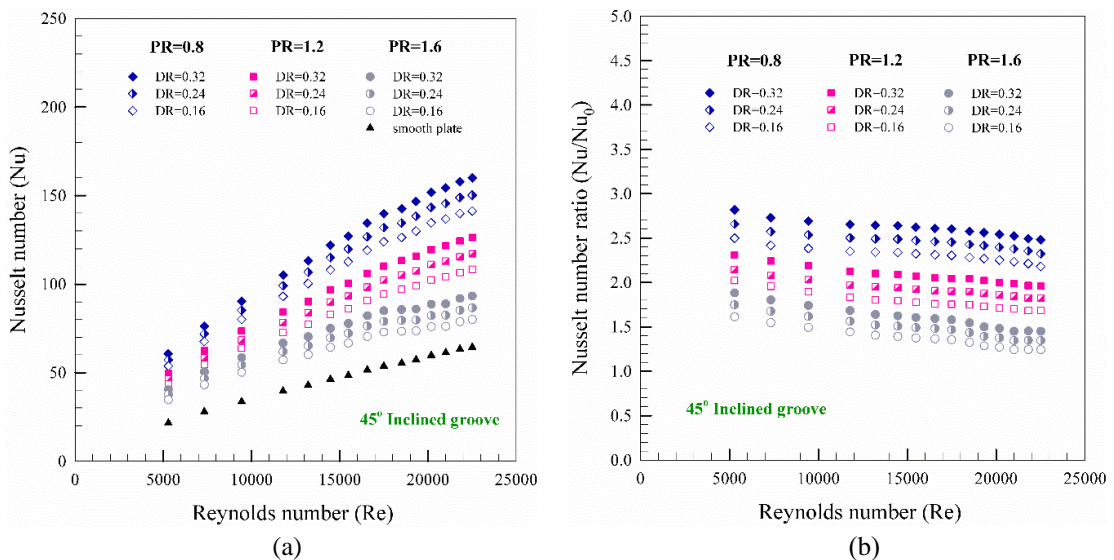

Fig. 6. Changes of (a) Nu and (b) Nu/Nu$_0$ in relation to Re for grooved absorber plate.

Figure 6(b) illustrates the relation between the enhanced Nu (Nu/Nu_0) of the grooved absorber and the Nu of the smooth absorber plate, as Re is varied for various DR and PR values. In the graph, the ratio of Nu to Nu_0 exhibits a modest decrease as the Reynolds number grows for all scenarios. A decrease in PR results in a rise in Nu/Nu_0, whereas a decrease in DR causes the opposite effect. The presence of an inclined groove with DR = 0.32 and PR = 0.8 leads to a notably greater Nu/Nu_0 in comparison to the other cases. Consequently, the heat transmission between the flowing air and absorber wall is accelerated as a result of the greater strength of vortex, which disrupts the boundary layer on the absorber surface. For DR values of 0.32, 0.24 and 0.16, the average Nu/Nu_0 values for PR values of 0.8, 1.2 and 1.6 are around 2.61, 2.46 and 2.31; 2.08, 1.93 and 1.79; and 1.6, 1.49 and 1.37 times, respectively, depending on the value of Re. This implies that the inclined groove with a smaller PR and a larger DR contributes to a significantly higher Nu/Nu_0. Nevertheless, as illustrated in the subsequent section, this circumstance leads to a notably increased friction loss.

4.4 Friction loss

For various values of PR and DR, Figure 7(a) and (b) demonstrates the corresponding changes in f and f/f_0 with relation to Re. Figure 6(a) shows that the grooved absorber plate generates a much larger f value than the smooth one. It has been noted that the f values from the three DR and PR values exhibit a similar tendency and decrease as the Re and PR values increased. It appears that the inclined groove channel has a larger f value (89–684% bigger) than the smooth channel. The increased f in the SAH channel is primarily due to the stronger vortex flows, which are in addition to the increase in groove depth.

For all groove parameters, the f/f_0 increases as Re increases, as shown in Figure 7(b). Within the context of 45° inclined groove situations, the f augmentations are shown to be minimal at DR = 0.16 and PR = 1.6, and maximal at DR = 0.32 and PR = 0.8. At PR = 0.8, 1.2 and 1.6, the average f/f_0 values are approximately 7.58, 6.68 and 5.8 times; 4.94, 4.36 and 3.78 times; and 2.73, 2.41 and 2.1 times, respectively, for DR = 0.32, 0.24 and 0.16. Because there is less flow resistance when the groove depth value on the absorber plate is small, the friction factor is reduced.
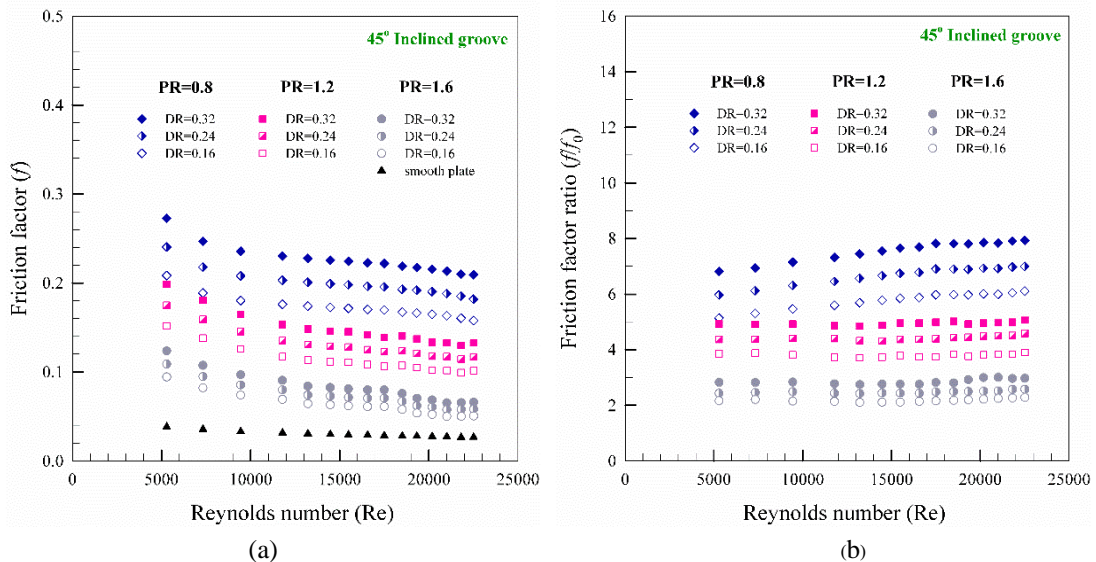

Fig. 7. Distributions of (a) f and (b) f/f_0 in relation to Re for grooved absorber plate.

4.5 Thermal performance

Figure 8 displays the relation between Re and TEF for various values of DR and PR. The TEF is calculated by taking the values of heat transmission and frictional loss at equal pumping power of the grooved and smooth absorber plates, as denoted in Eq. (12). As observed in the image, TEF has a tendency to drop as Re increases for all groove parameters. For DR=0.32, 0.24 and 0.16, the TEF values are as follows: 1.41–1.64, 1.37–1.6, 1.34–1.57; 1.26–1.47, 1.21–1.41, 1.16–1.38; and 1.13–1.36, 1.1–1.31, 1.04–1.26 at PR=0.8, 1.2 and 1.6, respectively. Clearly, the inclined groove with DR=0.32 and PR=0.8 has the maximum TEF of approximately 1.64. On average, this value is 10-27% larger than the devices studied in the prior research [25-28]. To obtain optimum thermal performance in the SAH system, the ideal choice for this inclined groove roughness is DR = 0.32 and PR = 0.8.
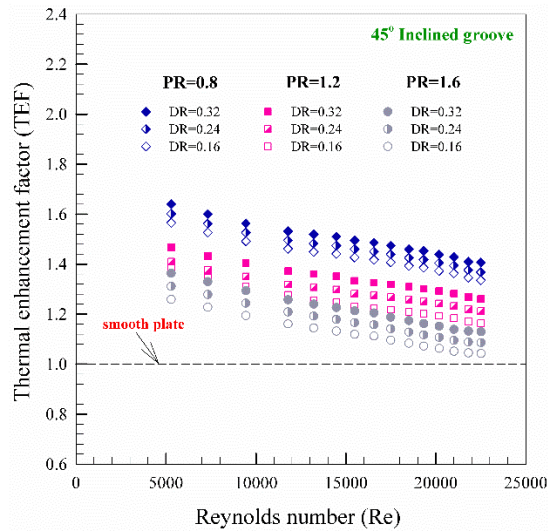
Fig. 8. TEF variation with Re for various inclined grooves.

5. Empirical correlations

The Nu and f correlations for the absorber plate with inclined grooves are established using experimental data. The relationships of these parameters are represented by equations (17) and (18), which illustrate their correlation. The correlations for Nu and f are represented as functions of DR, PR, Re and Pr (Prandtl number). Nevertheless, f is not influenced by Pr values, as demonstrated below:

$$\mathrm{Nu} = 0.297 \, \mathrm{Re}^{0.776} \mathrm{Pr}^{0.4} (\mathrm{DR})^{0.723} (\mathrm{PR})^{-0.228} \tag{17}$$

$$f = 10.65 \, \mathrm{Re}^{0.173} (\mathrm{DR})^{0.935} (\mathrm{PR})^{-0.617} \tag{18}$$

To assess the reliability of both correlations, the Nu and f values generated by the predicted correlations are contrasted to the measured data. This comparison is shown in Figure 9(a) and (b) for Nu and f values, respectively. The graph illustrates that most of the measurements are gathered within a range of ±8% for the predicted Nu, and ±10% for the anticipated f.
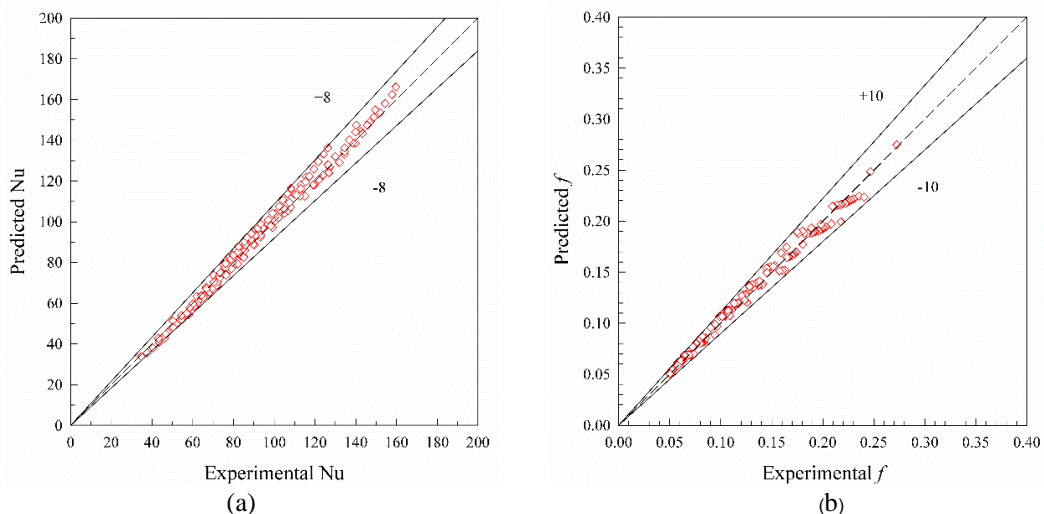

(a)　　　　　(b)

Fig. 9. Contrasts of experimental with estimated values for (a) Nu and (b) f.

6. Conclusions

An experimental work was carried out to figure out the influence of surface roughness, specifically a grooved absorber plate, on the transmission of heat and loss of flow friction in a SAH channel. The present work provides valuable insights into the impact of groove parameters, such as DR (depth ratio) and PR (pitch ratio), on thermal performance. The study focuses on turbulent flow conditions, namely within the range of Re from 5290 to 22,600. The investigation results in the following significant discoveries:

- Utilizing artificial roughness in the form of a groove has a major effect on the development of swirling flow inside a SAH channel, resulting in increased Nu as well as f.
- The heat transmission of all the characteristics of the grooved absorber plate is greatly improved compared to the smooth absorber plate. The Nu/Nu_0 ratio ranges from 1.24 to 2.82, whereas the f/f_0 ratio fluctuates between 1.88 and 7.9, depending upon the values of Re, PR and DR.
- The optimal thermal effectiveness factor (TEF) of approximately 1.64 is attained with DR = 0.32, PR = 0.8 and Re = 5290. Consequently, artificial roughness in a 45° inclined groove presents an achievable strategy for enhancing the effectiveness of a SAH system. The grooved absorber exhibits a markedly greater TEF than the smooth absorber, ranging from 4.3-64%.
- The correlations and the measured data agree quite well with one another.

References

[1]   Tamna S, Skullong S, Thianpong C, Promvonge P. Heat transfer behaviors in a solar air heater channel with multiple V-baffle vortex generators. Sol Energy. 2014;110:720–735.
[2]   Naphon P, Wiriyasart S. Investigation on performance analysis of a small solar electric generator. Case Stud Therm Eng. 2021;27:101224.
[3]   Skullong S, Promvonge P, Jayranaiwachira N, Thianpong C. Experimental and numerical heat transfer investigation in a tubular heat exchanger with delta-wing tape inserts. Chem Eng Process Process Intensif. 2016;109:164–177.
[4]   Koolnapado N, Hoonpong P, Skullong S, Kammul P, Promvonge P. Turbulent heat transfer and pressure loss in a square-duct heat exchanger with inclined-baffle inserts. Eng J. 2017;21:485–497.
[5]   Kwankaomeng S, Promvonge P. Numerical prediction on laminar heat transfer in square duct with 30° angled baffle on one wall. Int Commun Heat Mass Transf. 2010;37:857–866.
[6]   Promvonge P, Skullong S. Heat transfer in a tube with combined V-winglet and twin counter-twisted tape. Case Stud Therm Eng. 2021;26:101033.
[7]   Jayranaiwachira N, Promvonge P, Thianpong C, Skullong S. Entropy generation and thermal performance of tubular heat exchanger fitted with louvered corner-curved V-baffles. Int J Heat Mass Transf. 2023;201:123638.
[8]   Skullong S. Performance enhancement in a solar air heater duct with inclined ribs mounted on the absorber. J Res Appl Mech Eng. 2017;5:55–64.
[9]   Hoonpong P, Skullong S. Performance improvement of solar air heater with v-baffles on absorber plate. J Res Appl Mech Eng. 2018;6:29–39.
[10]   Promthaisong P, Skullong S. Thermal characterization in circular tube inserted with diamond-shaped rings. J Res Appl Mech Eng. 2019;7:1–10.
[11]   Bisht YS, Pandey SD, Chamoli S. Experimental investigation on jet impingement heat transfer analysis in a channel flow embedded with V-shaped patterned surface. Energy Sources Part A. 2023;45:12520–12534.
[12]   Singh H, Kishore C, Chamoli S, Joshi A. Enhancing heat transfer in rectangular solar air heater channels: a numerical exploration of multiple Boomerang-shaped roughness elements with variable gaps. Energy Sources Part A. 2024;46:6696–6712.
[13]   Lertnuwat B. Effect of the number and placement of punched holes in rectangular winglet vortex generators on solar air heater performance. Energy Convers Manage X. 2024;24:100714.
[14]   Promvonge P, Thianpong C, Jayranaiwachira N, Nakhchi ME, Skullong S. Effect of trapezoidal louvered winglets on increased heat transfer and exergy in tubular heat exchanger. Int J Therm Sci. 2024;204:109214.
[15]   Promvonge P, Jayranaiwachira N, Promthaisong P, Nakhchi ME, Skullong S. Thermal effectiveness analysis of heat exchange tube with staggered louver-punched V-baffles. Int Commun Heat Mass Transf. 2024;159:108052.

[16] Tang XY, Zhu DS. Flow structure and heat transfer in a narrow rectangular channel with different discrete rib arrays. Chem Eng Process Process Intensif. 2013;69:1–14.

[17] Promvonge P, Khanoknaiyakarn C, Sripattanapipat S, Skullong S. Heat transfer in solar air duct with multi-V-ribbed absorber and grooved back-plate. Chem Eng Res Des. 2021;168:84–95.

[18] Jayranaiwachira N, Promvonge P, Thianpong C, Skullong S. Thermal-hydraulic performance of solar receiver duct with inclined punched-ribs and grooves. Case Stud Therm Eng. 2022;39:102437.

[19] Taslim ME, Li T, Kercher DM. Experimental heat transfer and friction in channels roughened with angled, V-shaped, and discrete ribs on two opposite walls. ASME J Turbomach. 1996;118:20–28.

[20] Yadav AS, Bhagoria JL. A CFD based thermo-hydraulic performance analysis of an artificially roughened solar air heater having equilateral triangular sectioned rib roughness on the absorber plate. Int J Heat Mass Transf. 2014;70:1016–1039.

[21] Kumar A, Saini RP, Saini JS. Development of correlations for Nusselt number and friction factor for solar air heater with roughened duct having multi v-shaped with gap rib as artificial roughness. Renew Energy. 2013;58:151–163.

[22] Rashidi S, Hormozi F, Sundén B, Mahian O. Energy saving in thermal energy systems using dimpled surface technology – A review on mechanisms and applications. Appl Energy. 2019;250:1491–1547.

[23] Sethi M, Varun, Thakur NS. Correlations for solar air heater duct with dimpled shape roughness elements on absorber plate. Sol Energy. 2012;86:2852–2861.

[24] Jin DX, Lee YP, Lee DY. Effects of the pulsating flow agitation on the heat transfer in a triangular grooved channel. Int J Heat Mass Transf. 2007;50:3062–3071.

[25] Eiamsa-ard S, Promvonge P. Numerical study on heat transfer of turbulent channel flow over periodic grooves. Int Commun Heat Mass Transf. 2008;35:844–852.

[26] Luo L, Wen F, Wang L, Sundén B, Wang S. On the solar receiver thermal enhancement by using the dimple combined with delta winglet vortex generator. Appl Therm Eng. 2017;111:586–598.

[27] Chokphoemphun S, Hongkong S, Thongdaeng S, Chokphoemphun S. Experimental study and neural networks prediction on thermal performance assessment of grooved channel air heater. Int J Heat Mass Transf. 2020;163:120397.

[28] Zhang F, Liao G, Sundén B. Numerical investigations on the effect of convex-dimple streamwise arrangements on the flow and heat transfer characteristics of rectangular convex-dimple-grooved channels. Numer Heat Transf Part A. 2020;78:443–460.

[29] ASME. Standard Measurement of Fluid Flow in Pipes Using Orifice, Nozzle and Venturi. ASME MFC-3 M-1984. New York: United Engineering Center; 1984:1–56.

[30] Promvonge P, Skullong S. Thermal-hydraulic performance enhancement of solar receiver channel by flapped V-baffles. Chem Eng Res Des. 2022;182:87–97.

[31] Promvonge P, Promthaisong P, Skullong S. Experimental and numerical thermal performance in solar receiver heat exchanger with trapezoidal louvered winglet and wavy groove. Sol Energy. 2022;236:153–174.

[32] Moffat RJ. Describing the uncertainties in experimental results. Exp Therm Fluid Sci. 1988;1:3–17.

[33] Incropera FP, Witt PD, Bergman TL, Lavine AS. Fundamentals of Heat and Mass Transfer. Hoboken, NJ: John Wiley & Sons; 2006.